

Iron single-atom anchored N-doped carbon: An efficient catalyst for the one-pot, scale-up pentazolate synthesis

Pengbo Wang, Xiaopeng Zhang, Shuaijie Jiang, Zheting Dong, Ruyi Lu, Yuangang Xu, Pengcheng Wang*, Guo-Ping Lu*

School of Chemistry and Chemical Engineering, Nanjing University of Science & Technology, Xiaolingwei 200, Nanjing 210094, P. R. China.

* Corresponding authors: glu@njust.edu.cn; alexwpch@njust.edu.cn

1 General

All chemical reagents are obtained from commercial suppliers and used without further purification. XRD analysis was performed on Shimadzu X-ray diffractometer (XRD-6000) with Cu K α irradiation. Transmission electron microscopy (TEM) images were taken using a PHILIPS Tecnai 12 microscope operating at 120 kv. Atomic-resolution HAADF-STEM images were taken using a FEI Titan Cubed Themis G2 300 S/TEM with a probe corrector and a monochromator at 200 kV. X-ray photoelectron spectroscopy (XPS) was performed on an ESCALAB 250Xi spectrometer, using an Al K α X-ray source (1350 eV of photons) and calibrated by setting the C 1s peak to 284.80 eV. Inductively coupled plasma mass spectrometry (ICP-MS) was analyzed on Optima 7300 DV. BET surface area and pore size measurements were performed with N₂ adsorption/desorption isotherms at 77 K on a Micromeritics ASAP 2020 instrument. Before measurements, the samples were degassed at 150 °C for 12 h. The X-ray absorption spectra (XAS) including X-ray absorption near-edge structure (XANES) and extended X-ray absorption fine structure (EXAFS) of the samples at Fe K-edge (7712 eV) were collected at the Singapore Synchrotron Light Source (SSLS) center, where a pair of channel-cut Si (111) crystals was used in the monochromator. The Fe K-edge XANES data were recorded in a transmission mode. Fe foil, Fe₂O₃ and FePc were used as references. The storage ring was working at the energy of 2.5 GeV with an average electron current of below 200 mA. The acquired EXAFS data were extracted

and processed according to the standard procedures using the ATHENA module implemented in the IFEFFIT software packages. Electron paramagnetic resonance (EPR) spectra were from Bruker A300. Anion chromatograms was performed on the Thermo Scientific Dionex ICS-6000 DP. Infrared spectrum was measured by Thermo Scientific Nicolet iS50 FTIR at a scan rate of 4 cm⁻¹/s. High-resolution mass spectrum was derived from Ultimate 3000 UHPLC-Q Exactive.

2 Catalyst preparation

2.1 Synthesis of NC-x (x means pyrolysis temperature)

First, melamine and carbon black were thoroughly mixed through grinding and placed in the tube furnace. Subsequently, the mixture was heated at 700 °C for 2 h under N₂ atmosphere with a heating rate of 5 °C·min⁻¹ to afford NC-700. NC-800 and NC-900 were also synthesized by similar procedure except for different pyrolysis temperatures.

2.2 Synthesis of Fe₁@NC-x, Fe₂@NC-x and Co@NC-x

Fe₁@NC-x: First, FeSO₄·7H₂O was dissolved in deionized water. The obtained solution and NC-x support are added into a ball milling tank (250 mL). After adding 50 agate balls (3 mm diameter) into the tank, it was placed in a ball mill and ground at 100 W power for 4 h. The obtained solid was centrifuged, washed with water and dried under vacuum to produce the final catalyst (Fe₁@NC-x).

Fe₁@NC-700-2, Co₁@NC-700: The synthesis steps are the same as Fe₁@NC-x except for replacing FeSO₄·7H₂O with an equal molar amount of FeCl₃ or CoSO₄·7H₂O.

2.3 Catalytic reactions

The general procedure for the synthesis of NaN₅

2,6-Dimethyl-4-aminophenol hydrochloride **1** (15.10 g, 87 mmol) was added to the tetrahydrofuran (50 mL) and magnetically stirred. After the solid was completely dissolved, a dose of hydrochloric acid (36 wt.%, 8 mL, 96 mmol) was added. Then, sodium nitrite (6.21 g, 90 mmol) aqueous solution was added dropwise slowly at -5 °C.

After 30 min, 100 mL pre-cooled methanol was added and the reaction system was cooled to $-40\text{ }^{\circ}\text{C}$, and then sodium azide (5.85 g, 90 mmol) aqueous solution was added dropwise slowly. The resulting mixture was stirred at $-40\text{ }^{\circ}\text{C}$ for 2 h, and pre-cooled acetonitrile (100 mL) was added. After 10 min, $\text{Fe}_1\text{@NC-700}$ was added to the mixture. After 30 min, 3-chloroperbenzoic acid (*m*CPBA, 85 wt.%) was added in portions. The reaction mixture slowly heated up to $-15\text{ }^{\circ}\text{C}$ and continued to react at the same temperature for 12 h.

After the reaction was completed, the mixture was filtered to remove iron catalyst. The resulted filtrate was concentrated by rotary evaporation at room temperature. When most of the mixed organic solvent in the reaction solution was removed, a small amount of water was added to make N_5^- fully dissolved in the aqueous phase. Then the precipitated solid were filtered out, and the filtrate was extracted by ethyl acetate to remove the residual organic compounds in the filtrate. After removing the aqueous phase, a white solid was obtained, which was then redissolved in ethanol to filter out the insoluble inorganic salt impurities. The crude product was then further purified by silica gel column chromatography (ethanol/ethyl acetate) to afford a white solid (NaN_5).

The procedure for the synthesis of CoN_5

The one-pot three-step process for the preparation of CoN_5 was the same as that of NaN_5 , but the purification procedure of CoN_5 differs from that of NaN_5 . Herein, we only introduces the post-treatment process of CoN_5 .

After the reaction was completed, the reaction mixture was filtered to remove iron catalyst. When most of the filtrate was removed by rotary evaporation, some water was added and then the sediment was filtered. Hydrochloric acid (1 M) was used to adjust the pH of filtrate to about 3~4. Then, a large amount of ethyl acetate was used to remove organic matter in the filtrate by extraction. The aqueous phase was concentrated by rotary evaporation to filter white solid precipitates. Co(II) salt was added to the filtrate and stirred at room temperature to form CoN_5 precipitates, which was washed with ethyl acetate and water to obtain CoN_5 .

Catalyst recycling

After the reaction was completed, the catalyst can be separated by filtration, which

could be reused in the next run after washing by ethanol and water to remove adsorbed organic matter and salts.

2.4 Preparation processes for the scale-up synthesis of pentazolates

The procedure for the NaN_5 synthesis catalyzed by $\text{Fe}(\text{Gly})_2$

2,6-Dimethyl-4-aminophenol hydrochloride **1** (302 g, 1.74 mol) was added to the tetrahydrofuran (1 L) under mechanical stirring. After the solid was completely dissolved, a dose of hydrochloric acid (36 wt.%, 160 mL, 1.92 mol) was added. Then, sodium nitrite (124.2 g, 1.80 mol) aqueous solution was added dropwise slowly at -5°C , and the mixture continued to react for 1 h. The reaction system was cooled to -40°C after pre-cooled methanol (2 L) was added. After sodium azide (117 g, 1.80 mol) aqueous solution was added dropwise slowly, the resulting mixture was stirred at -40°C for 2 h. The reaction mixture was extracted and filtered at -60°C , and the filter residue was washed with pre-cooled acetone to obtain **2**.

Then, All **2** and 850 g $\text{Fe}(\text{Gly})_2$ were added sequentially to the pre-cooled acetonitrile under mechanical stirring at -40°C . After 1 h, 3-chloroperbenzoic acid (*m*CPBA, 660 g, 85 wt.%) was added in portions, and the reaction mixture slowly heated up to -15°C and continued to react at the same temperature for 12 h.

After the reaction was completed, the mixture was filtered to remove iron catalyst. The resulted filtrate was concentrated by rotary evaporation at room temperature. When most of the mixed organic solvent in the reaction solution was removed, a small amount of water was added to make N_5^- fully dissolved in the aqueous phase. Then the precipitated solid were filtered out, and the filtrate was extracted by ethyl acetate to remove the residual organic compounds in the filtrate. After removing the aqueous phase, a white solid was obtained, which was then redissolved in ethanol to filter out the insoluble inorganic salt impurities. The crude product was then further purified by silica gel column chromatography (ethanol/ethyl acetate) to afford a white solid (NaN_5).

The procedure for the NaN_5 synthesis catalyzed by $\text{Fe}_1@\text{NC-700}$

2,6-Dimethyl-4-aminophenol hydrochloride **1** (302 g, 1.74 mol) was added to the tetrahydrofuran (1 L) under mechanical stirring. After the solid was completely dissolved, a dose of hydrochloric acid (36 wt.%, 160 mL, 1.92 mol) was added. Then,

sodium nitrite (124.2 g, 1.80 mol) aqueous solution was added dropwise slowly at -5 °C, and the mixture continued to react for 1 h. The reaction system was cooled to -40 °C after pre-cooled methanol (2 L) and sodium azide (117 g, 1.80 mol, dropwise) aqueous solution were added. The resulting mixture was stirred at -40 °C for 2 h and pre-cooled acetonitrile (2 L) was added. After 1 h, Fe₁@NC-700 (80 g) was added to the mixture. After 1 h, 3-chloroperbenzoic acid (*m*CPBA, 660 g, 85 wt.%) was added in portions. The reaction mixture slowly heated up to -15 °C and continued to react at the same temperature for 12 h.

After the reaction was completed, the mixture was filtered to remove iron catalyst. The resulted filtrate was concentrated by rotary evaporation at room temperature. When most of the mixed organic solvent in the reaction solution was removed, a small amount of water was added to make N₅⁻ fully dissolved in the aqueous phase. Then the precipitated solid were filtered out, and the filtrate was extracted by ethyl acetate to remove the residual organic compounds in the filtrate. After removing the aqueous phase, a white solid was obtained, which was then redissolved in ethanol to filter out the insoluble inorganic salt impurities. The crude product was then further purified by silica gel column chromatography (ethanol/ethyl acetate) to afford a white solid (NaN₅).

The procedure for the synthesis of CoN₅ by Fe₁@NC-700

2,6-Dimethyl-4-aminophenol hydrochloride **1** (302 g, 1.74 mol) was added to the tetrahydrofuran (1 L) and mechanical agitation. After the solid was completely dissolved, a dose of hydrochloric acid (36 wt.%, 160 mL, 1.92 mol) was added. Then, sodium nitrite (124.2 g, 1.80 mol) aqueous solution was added dropwise slowly at -5 °C. After 1 h, pre-cooled methanol (2 L) was added and the reaction system was cooled to -40 °C, and then sodium azide (117 g, 1.80 mol) aqueous solution was added dropwise slowly. The resulting mixture was stirred at -40 °C for 2 h, and pre-cooled acetonitrile (2 L) was added. After 1 h, Fe₁@NC-700 (80 g) was added to the mixture. After 1 h, 3-chloroperbenzoic acid (*m*CPBA, 660 g, 85 wt.%) was added in portions. The reaction mixture slowly heated up to -15 °C and continued to react at the same temperature for 12 h.

After the reaction was completed, the reaction mixture was filtered to remove iron

catalyst. When most of the filtrate was removed by rotary evaporation, some water was added and then the sediment was filtered. Hydrochloric acid (1 M) was used to adjust the pH of filtrate to about 3~4. Then, a large amount of ethyl acetate was used to remove organic matter in the filtrate by extraction. The aqueous phase was concentrated by rotary evaporation to filter white solid precipitates. Co(II) salt was added to the filtrate and stirred at room temperature to form CoN_5 precipitates, which was washed with ethyl acetate and water to obtain CoN_5 .

3 Computational Details

All geometry optimizations were performed at the density functional theory (DFT) level using the TPSS function^[1] with basis set 6-31G(d)^[2] for the nonmetallic atoms and SDD^[3] for Fe. The Grimme's D3 dispersion correction^[4] using the Becke-Johnson damping function^[5] was employed in the calculations to appropriately evaluate the intermolecular interactions. The nature of the optimized stationary points was characterized by the frequency calculations at the same level of theory, with all reactant (R), intermediate (IM) and product (P) configurations having no imaginary frequency, and all transition states (TSs) having one imaginary mode. Thermal corrections to the electronic energies of the optimized geometries were estimated at the experimental temperature 263 K and 1 atm from the frequency calculations. The intrinsic reaction coordinate (IRC)^[6] calculations from the first-order saddle points were performed to locate the local minima for the reaction pathways, which are denoted by solid lines in the energy profile. Solvent effects were implicitly taken into account by means of solvation model based on density (SMD) method^[7] with $\epsilon = 34.15$ ($\text{CH}_3\text{OH}/\text{CH}_3\text{CN} = 1/1$). To obtain more accurate electronic energies as well as reaction barrier heights, we further carried out single point calculations based on the optimized geometries by using the PBE0 function^[8] with larger basis sets 6-311+g(d,p)/SDD^[9] for the nonmetallic/Fe atoms. All calculations were performed using Gaussian 09 E.01 suite of program.^[10]

4 Single-crystal X-ray diffraction analysis

The Crystal data of $[\text{Co}(\text{H}_2\text{O})_4(\text{N}_5)_2] \cdot 4\text{H}_2\text{O}$ were collected with a Bruker D8 Venture single-crystal. The crystal was kept at 193.00 K during data collection. Using Olex2,

the structure was solved with the olex2. solve structure solution program using Charge Flipping and refined with the SHELXL refinement package using Least Squares minimization diffractometer.

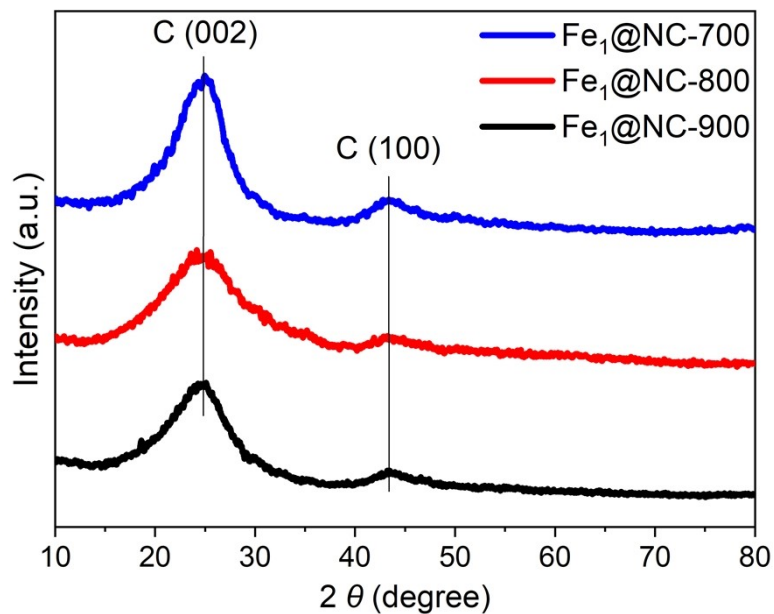


Figure S1 Powder XRD patterns of Fe₁@NC-x catalysts.

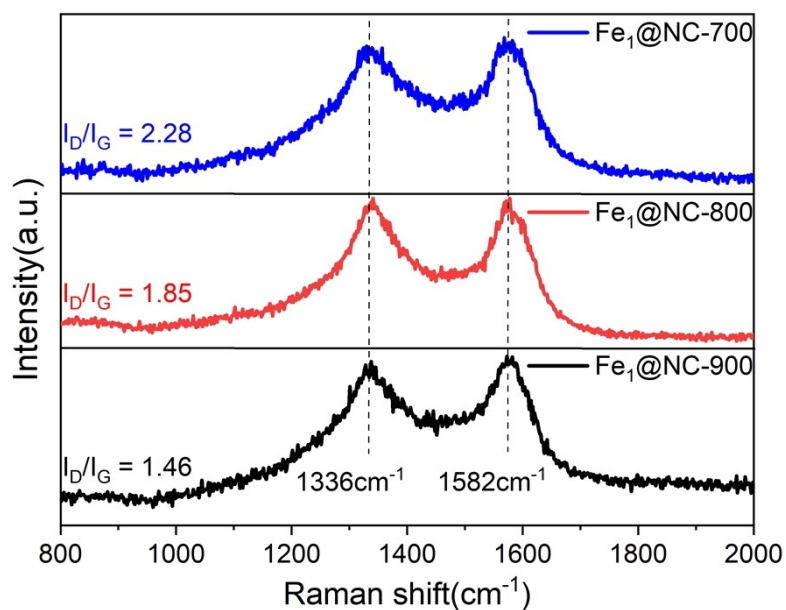


Figure S2 Raman spectra of Fe₁@NC-x catalysts.

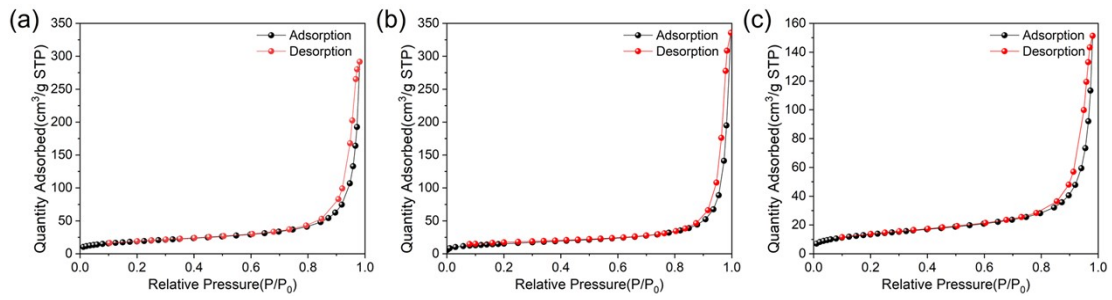


Figure S3 Nitrogen isotherm adsorption/desorption of (a) Fe₁@NC-700, (b) Fe₁@NC-800 and (c) Fe₁@NC-900.

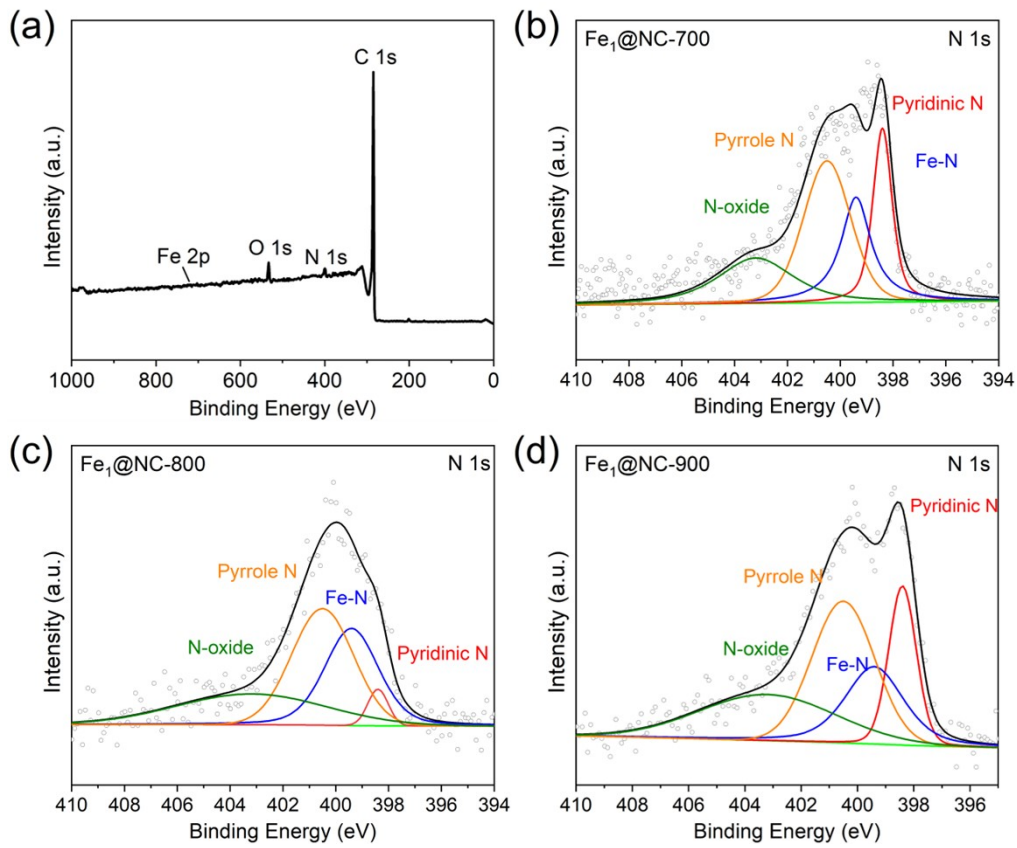


Figure S4 (a) XPS survey spectrum of Fe₁@NC-700, (b) N 1s spectra of Fe₁@NC-700, (c) N 1s spectra of Fe₁@NC-800, (d) N 1s spectra of Fe₁@NC-900

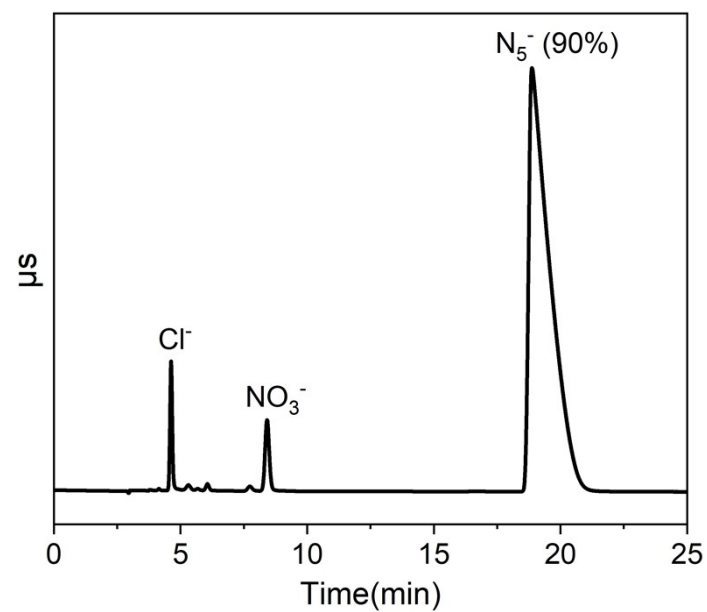


Figure S5 Anion chromatogram of NaN_5

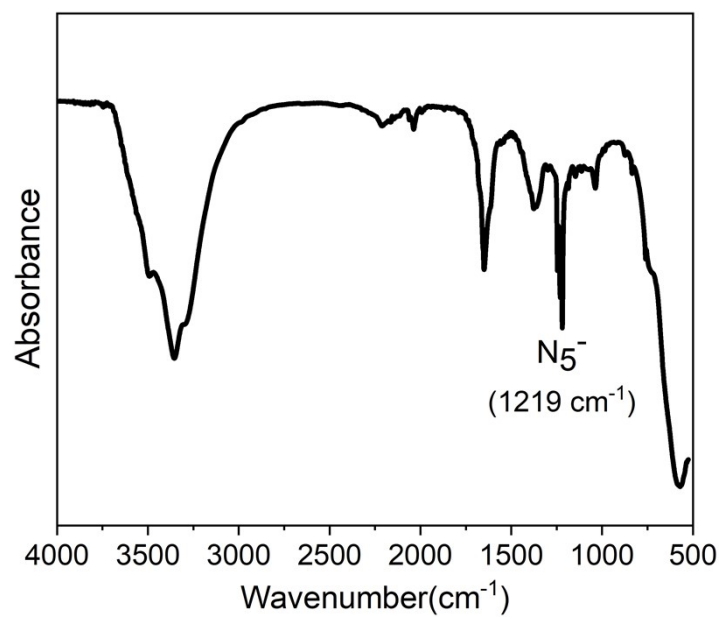


Figure S6 Infrared spectra of NaN_5

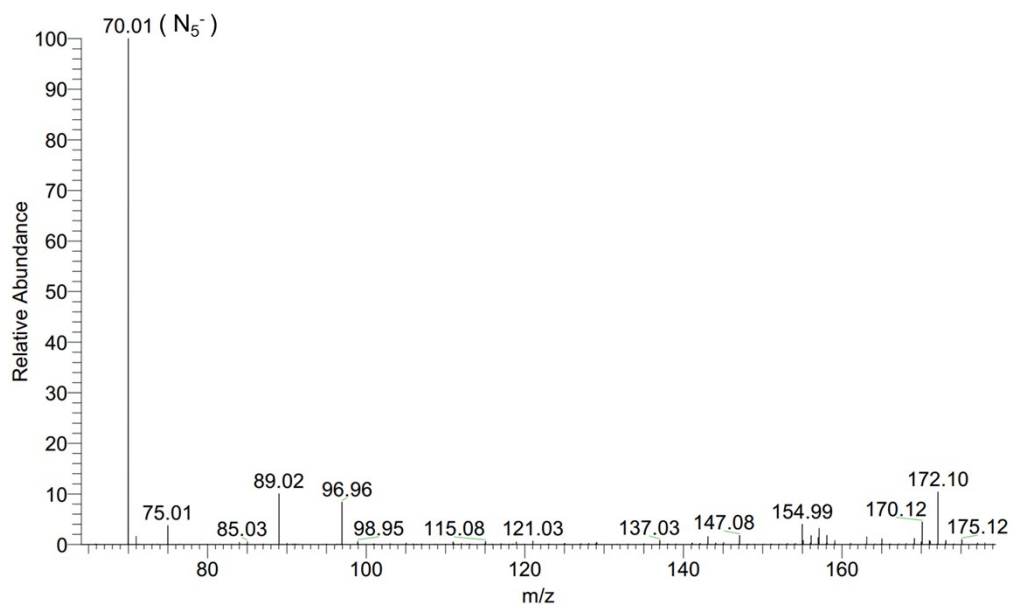


Figure S7 Mass spectrum of NaN_5

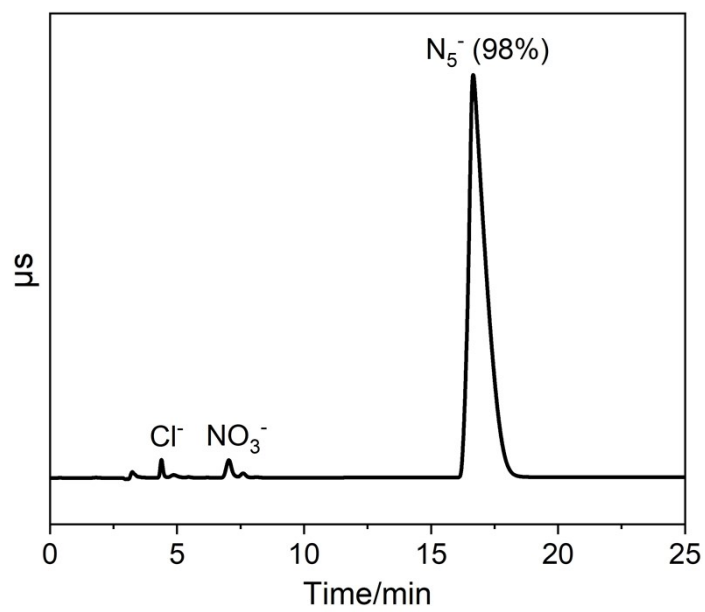


Figure S8 Anion chromatogram of CoN_5

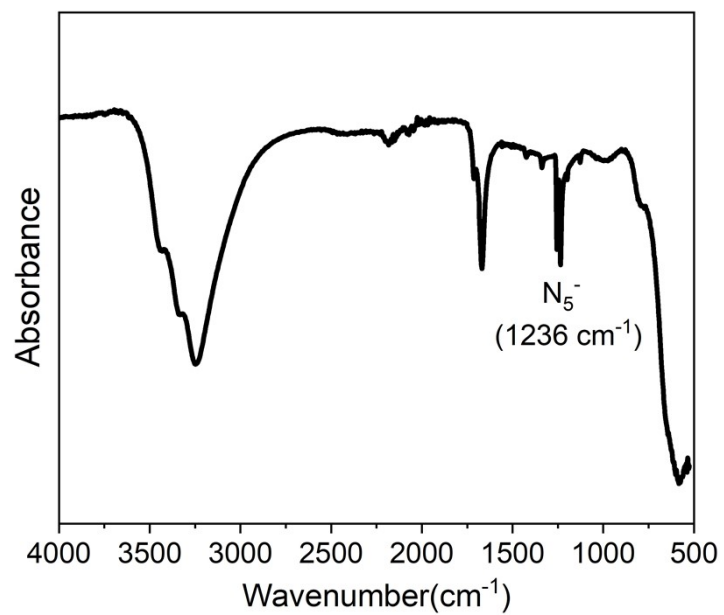


Figure S9 Infrared spectra of CoN₅

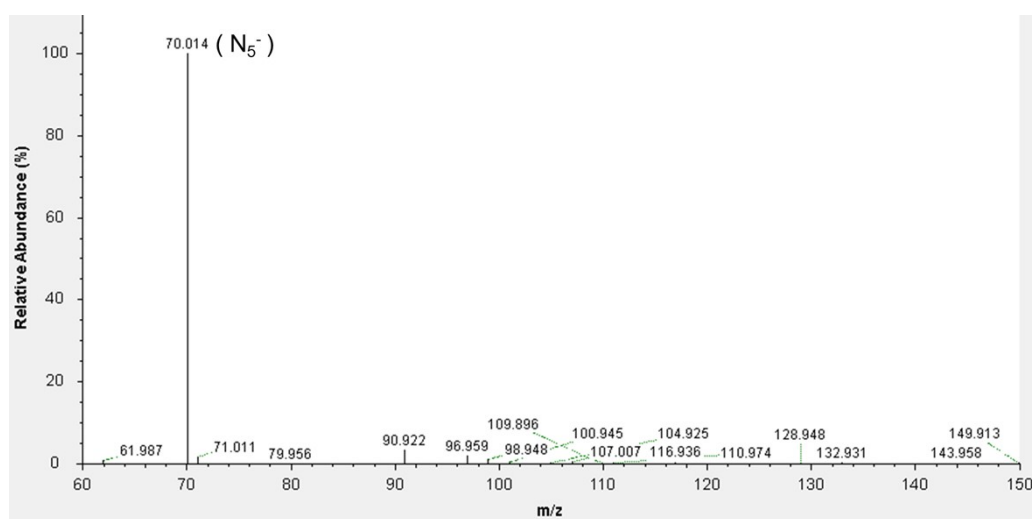


Figure S10 Mass spectrum of CoN₅

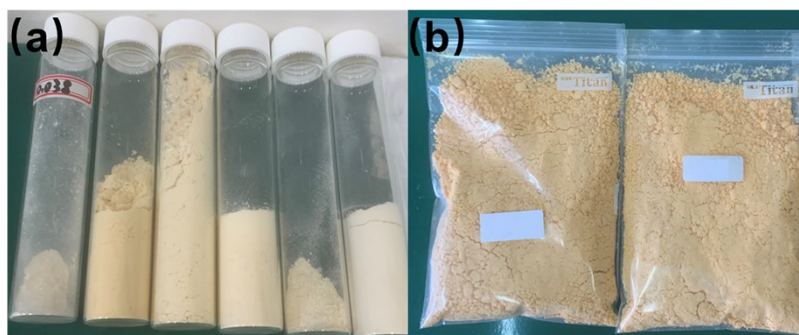


Figure S11 Image of NaN₅ (a) and CoN₅ (b)

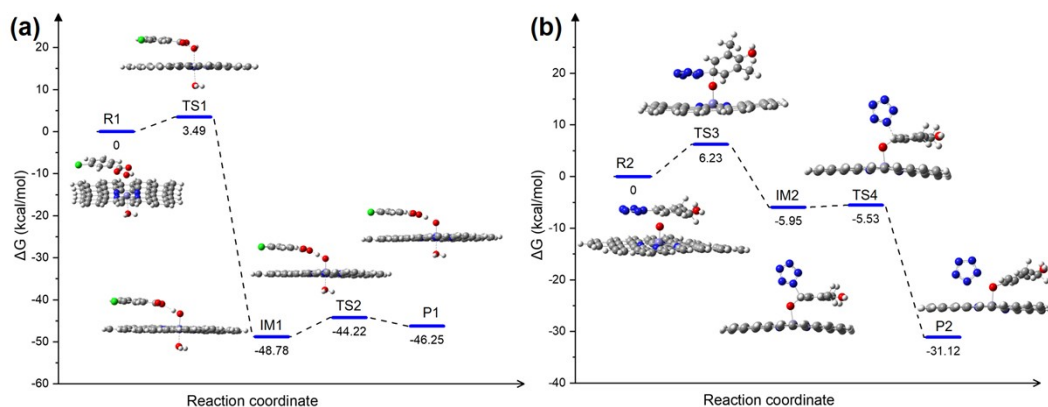


Figure S12 (a) Gibbs free-energy profile for the reaction of FeN₄ (calculation model of Fe₁@NC-700) with *m*CPBA. (b) Gibbs free-energy profile for the reaction of arylpentazole **2** with Fe(IV)=O intermediate. Silvery, grey, dark blue, red, green and light blue balls represent hydrogen, carbon, nitrogen, oxygen, chlorine and iron atoms, respectively.

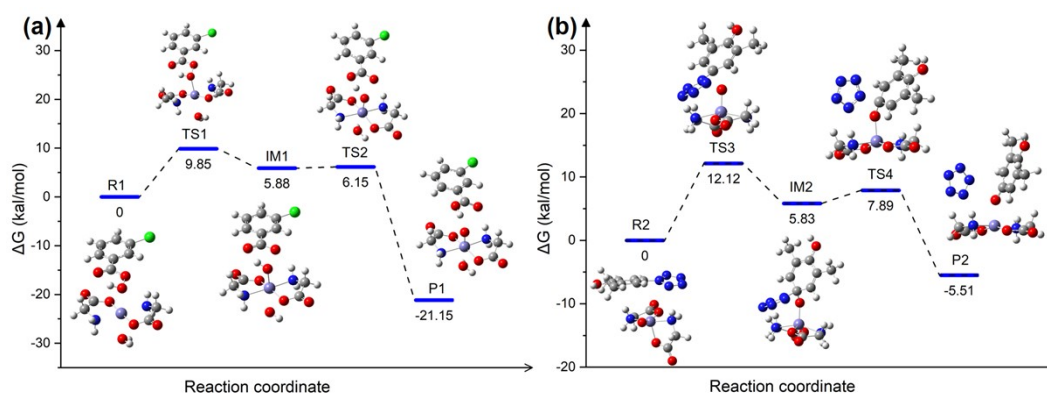


Figure S13 (a) Gibbs free-energy profile for the reaction of Fe(Gly)₂ with *m*CPBA. (b) Gibbs free-energy profile for the reaction of arylpentazole **2** with Fe(IV)=O intermediate. Silvery, grey, dark blue, red, green and light blue balls represent hydrogen, carbon, nitrogen, oxygen, chlorine and iron atoms, respectively.

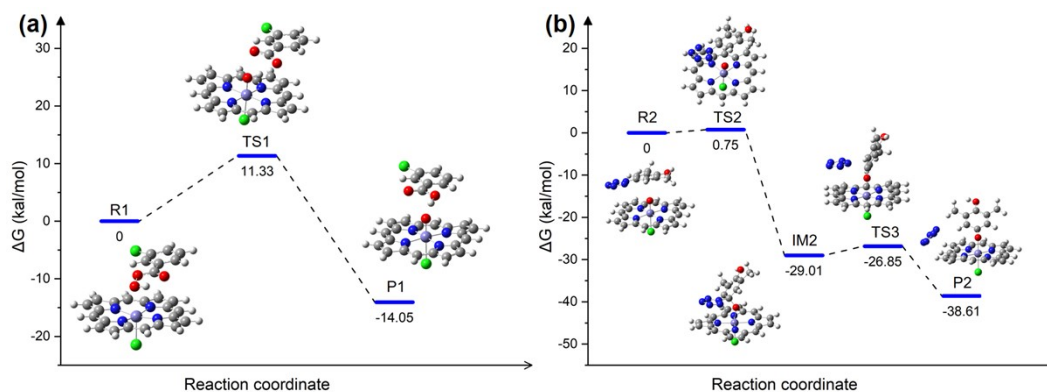


Figure S14 (a) Gibbs free-energy profile for the reaction of Hemin with *m*CPBA. (b) Gibbs free-energy profile for the reaction of arylpentazole **2** with Fe(IV)=O intermediate. Silvery, grey, dark blue, red, green and light blue balls represent hydrogen, carbon, nitrogen, oxygen, chlorine and iron atoms, respectively.

Table S1 The iron content of Fe₁@NC-x based on ICP-MS.

Samples	Fe ₁ @NC-700	Fe ₁ @NC-800	Fe ₁ @NC-900
Metal contents (wt.%)	0.82	0.73	0.65

Table S2 The BET surface area and average pore size of the Fe₁@NC-x.

Catalyst	BET surface area (m ² /g)	Average pore size (nm)
Fe ₁ @NC-700	68.41	38.56
Fe ₁ @NC-800	55.43	28.99
Fe ₁ @NC-900	48.95	23.13

Table S3 The relative concentrations of different N species based on XPS of the Fe₁@NC-x.

Catalyst	Total N (atom %)	Relative concentrations of different N species (area %)			
		Pyridinic N	Fe-N	Pyrrole N	N-oxide
Fe ₁ @NC-700	3.80	20.54	22.80	35.35	21.31
Fe ₁ @NC-800	3.42	3.36	21.72	38.17	36.75
Fe ₁ @NC-900	3.17	16.27	17.07	32.25	34.41

Table S4 EXAFS fitting parameters at the Fe K-edge for various samples ($S_0^2=0.786$).

Sample	Shell	CN	R(Å)	$\sigma^2(\text{Å}^2)$	$\Delta E_0(\text{eV})$	R factor
Fe foil	Fe-Fe	8*	2.464±0.012	0.0047±0.0013	5.7±1.9	0.0066
	Fe-Fe	6*	2.849±0.010	0.0052±0.0021		
Fe ₁ @NC-700	Fe-N	3.9±0.3	2.050±0.006	0.0042±0.0037	-1.2±1.7	0.0098

C.N. : coordination numbers; R : bond distance; σ^2 : Debye-Waller factors; ΔE_0 : the inner potential correction. R factor : goodness of fit. * the experimental EXAFS fit of metal foil by fixing CN as the known crystallographic value.

Table S5 Crystallographic data for $\text{Co}(\text{H}_2\text{O})_4(\text{N}_5)_2 \cdot 4\text{H}_2\text{O}$

$\text{Co}(\text{H}_2\text{O})_4(\text{N}_5)_2 \cdot 4\text{H}_2\text{O}$	
Empirical formula	$\text{CoH}_{16}\text{N}_{10}\text{O}_8$
Formula weight	343.16
Temperature / K	193.00
Crystal system	orthorhombic
Space group	Fmmm
$a / \text{\AA}$	12.1491(6)
$b / \text{\AA}$	17.1419(9)
$c / \text{\AA}$	6.4555(4)
$\alpha / ^\circ$	90
$\beta / ^\circ$	90
$\gamma / ^\circ$	90
Volume / \AA^3	1344.41(13)
Z	4
$\rho_{\text{calc}} / \text{g cm}^{-3}$	1.695
μ / mm^{-1}	7.368
$F(000)$	708.00
Crystal size / mm^3	$0.13 \times 0.11 \times 0.1$
Radiation	GaK α ($\lambda = 1.34139$)
2θ range for data collection/ $^\circ$	8.976 to 107.798
Index ranges	$-14 \leq h \leq 14, -20 \leq k \leq 18, -7 \leq l \leq 7$
Reflections collected	3889
Independent reflections	371 [$R_{\text{int}} = 0.0610, R_{\text{sigma}} = 0.0299$]
Data / restraints / parameters	371/1/39
Goodness-of-fit on F^2	1.19
Final R indexes [$I \geq 2\sigma(I)$]	$R_1 = 0.0282, wR_2 = 0.0653$
Final R indexes [all data]	$R_1 = 0.0283, wR_2 = 0.0655$
Largest diff. peak / hole / $e \text{\AA}^{-3}$	0.43/-0.36

Table S6. Bond lengths for $\text{Co}(\text{H}_2\text{O})_4(\text{N}_5)_2 \cdot 4\text{H}_2\text{O}$

Parameter	Bond length (\AA)	Parameter	Bond length (\AA)
Co(1)-O(1) ¹	2.0568(18)	Co(1)-N(1)	2.133(2)
Co(1)-O(1) ²	2.0568(18)	N(3)-N(1)	1.317(2)
Co(1)-O(1) ³	2.0568(18)	N(3)-N(2)	1.316(3)
Co(1)-O(1)	2.0568(18)	N(2)-N(2) ⁴	1.320(4)
Co(1)-N(1) ¹	2.133(2)		

¹1-X, 1-Y, 1-Z; ²+X, +Y, 1-Z; ³1-X, 1-Y, +Z; ⁴1-X, +Y, 1-Z.

Table S7 Bond angles for $\text{Co}(\text{H}_2\text{O})_4(\text{N}_5)_2 \cdot 4\text{H}_2\text{O}$

parameter	bond angle (°)	parameter	bond angle (°)
O(1) ¹ -Co(1)-O(1) ²	91.23(11)	O(1) ¹ -Co(1)-N(1) ¹	90.0
O(1) ² -Co(1)-O(1) ³	180.0	O(1)-Co(1)-N(1) ¹	90.0
O(1) ¹ -Co(1)-O(1) ³	88.77(11)	O(1)-Co(1)-N(1)	90.0
O(1) ² -Co(1)-O(1)	88.77(11)	O(1) ³ -Co(1)-N(1) ¹	90.0
O(1) ¹ -Co(1)-O(1)	180.0	N(1) ¹ -Co(1)-N(1)	180.0
O(1) ³ -Co(1)-O(1)	91.23(11)	N(2)-N(3)-N(1)	107.50(19)
O(1) ² -Co(1)-N(1)	90.0	N(3) ⁴ -N(1)-Co(1)	125.65(12)
O(1) ³ -Co(1)-N(1)	90.0	N(3)-N(1)-Co(1)	125.65(12)
O(1) ² -Co(1)-N(1) ¹	90.0	N(3)-N(1)-N(3) ⁴	108.7(2)
O(1) ¹ -Co(1)-N(1)	90.0	N(3)-N(2)-N(2) ⁴	108.15(13)

¹1-X, 1-Y, 1-Z; ²+X, +Y, 1-Z; ³1-X, 1-Y, +Z; ⁴1-X, +Y, 1-Z.

Table S8 Torsion angles for $\text{Co}(\text{H}_2\text{O})_4(\text{N}_5)_2 \cdot 4\text{H}_2\text{O}$

parameter	torsion angle (°)	parameter	torsion angle (°)
N(1)-N(3)-N(2)-N(2) ¹	0.0	N(2)-N(3)-N(1)-N(3) ¹	0.0
N(2)-N(3)-N(1)-Co(1)	180.0		

¹1-X, +Y, 1-Z.

Table S9 Hydrogen Atom Coordinates ($\text{Å} \times 10^4$) and Isotropic Displacement Parameters ($\text{Å}^2 \times 10^3$) for $\text{Co}(\text{H}_2\text{O})_4(\text{N}_5)_2 \cdot 4\text{H}_2\text{O}$

Atom	x	y	z	U(eq)
H(2A)	6403.1	6565.88	10000	46(8)
H(2B)	7461.1	6275.68	10000	43(8)
H(1)	6370(18)	5376(10)	7910(30)	55(7)

References

- [1] Stephens. P.; Devlin, F.; Chabalowski, C.; Frisch, M. Ab Initio Calculation of Vibrational Absorption and Circular Dichroism Spectra Using Density Functional Force Fields. *J. Phys. Chem.* **1994**, *98*, 11623-11627.
- [2] Hariharan, P.; Pople, J. The influence of polarization functions on molecular orbital hydrogenation energies. *Theor. Chim. Acta.* **1973**, *28*, 213-222.
- [3] Dolg, M.; Stoll, H.; Savin, A.; Preuss, H. Energy-adjusted pseudopotentials for the rare earth elements. *Theor. Chim. Acta.* **1989**, *90*, 1730-1734.
- [4] Grimme, S.; Antony, J.; Ehrlich, S.; Krieg, K. A consistent and accurate ab initio parametrization of density functional dispersion correction (DFT-D) for the 94 elements H-Pu. *J. Chem. Phys.* **2010**, *132*, 154104.
- [5] Grimme, S.; Ehrlich, S.; Goerigk, L. Effect of the damping function in dispersion corrected density functional theory. *J. Comput. Chem.* **2011**, *32*, 1456-1465.
- [6] Hratchian, H.; Schlegel, H. Using Hessian updating to increase the efficiency of a Hessian based predictor-corrector reaction path following method. *J. Chem. Theory Comput.* **2005**, *1*, 61-69.
- [7] Marenich, A.; Cramer, C.; Truhlar, D.; Universal solvation model based on solute electron density and on a continuum model of the solvent defined by the bulk dielectric constant and atomic surface tensions. *J. Phys. Chem. B.* **2009**, *113*, 6378-6396.
- [8] Adamo, C.; Barone, V. Toward reliable density functional methods without adjustable parameters: The PBE0 model. *J. Chem. Phys.* **1999**, *110*, 6158-6170.
- [9] Frisch, M.; Pople, J.; Binkley, J. Self-consistent molecular orbital methods 25. Supplementary functions for Gaussian basis sets. *J. Chem. Phys.* **1984**, *80*, 3265-3269.
- [10] Frisch, M.; Trucks, G.; Schlegel, H. Gaussian 09 Revision D.01. **2009**.